

RESULTS OF METALLOGRAPHIC ANALYSIS OF THE QUENCH-20 BUNDLE WITH B₄C ABSORBER

J. Stuckert, U. Peters, U. Stegmaier, M. Steinbrück

Karlsruhe Institute of Technology
Hermann-von-Helmholtz-Platz 1, 76344 Eggenstein-Leopoldshafen
juri.stuckert@kit.edu

ABSTRACT

Experiment QUENCH-20 with BWR geometry simulation bundle was conducted at KIT on 9th October 2019 in the framework of the international SAFEST project. The test bundle mock-up represented one quarter of a BWR fuel assembly with 24 electrically heated fuel rod simulators and two B₄C control blades. The rod simulators were filled with Kr to inner pressure of 5.5 bar at peak cladding temperature of 900 K. The pre-oxidation stage in the flowing gas mixture of steam and argon (each 3 g/s) and system pressure of 2 bar lasted 4 hours at the peak cladding temperature of 1250 K. During the following transient stage, the bundle was heated to a maximal temperature of 2000 K. The cladding radial extensions and failures due to inner overpressure (about 4 bar) were observed at temperature about 1700 K and lasted about 200 s. During the period of rod failures also the first absorber melt relocation accompanied by shroud failure were registered. The interaction of B₄C with steel blade and ZIRLO channel box was observed at elevations 650...950 mm with formation of eutectic melt. The typical components of this melt are (Fe, Cr) borides and ZrB₂ precipitated in steel or in Zr-steel eutectic melt. Massive absorber melt relocation was observed 50 s before the end of transition stage. Small fragments of the absorber melt moved down to the elevation of 50 mm. The test was terminated with the quench water injected with a flow rate of 50 g/s from the bundle bottom. Fast temperature escalation from 2000 to 2300 K during 20 s was observed. As result, the metal part (prior β -Zr) of claddings between 550 and 950 mm was melted, partially released into space between rods and partially relocated in the gap between pellet and outer oxide layer to 450 mm. The bundle elevations 850 and 750 mm are mostly oxidized with average cladding ECR 33%.

KEYWORDS

BWR test bundle, cladding oxidation, eutectic melt relocation, reflood, temperature escalation

1. INTRODUCTION

The main objective of the QUENCH program at KIT is the investigation of the hydrogen source term and materials interactions during LOCA and the early phase of severe accidents including reflood [1-3]. Bundle experiments as well as separate-effects tests are conducted to provide data for the development of models and the validation of severe fuel damage code systems. The QUENCH bundle facility is an out-of-pile bundle facility with electrically heated fuel rod simulators and extensive instrumentation. So far, 20 experiments with various severe accident scenarios as well as a series of 7 DBA LOCA experiments were conducted. Two of the bundle tests on severe accident were performed with PWR geometry containing central B₄C neutron absorber rod: QUENCH-07 [4] and QUENCH-09 [5]. Numerous accompanying single control rod tests were performed at KIT and showed a complicated eutectic interaction between B₄C, stainless steel and zirconium with formation of different borides [6, 7]. The last severe accident test QUENCH-20 was the first test performed in the QUENCH facility with BWR geometry simulation bundle [8].

2. TEST FACILITY

The general scheme of the test section is given in Fig. 1. The test rods were arranged within the bundle as shown in the schematic cross section of Fig. 2. The rod cladding of the fuel rod has 9.84 mm outside diameter and 8.63 mm inner diameter. The materials used in this test consisted of Zircaloy-2 cladding tubes with inner liner (LK3/L). The composition of the LK3 and L materials can be found in Table 3.

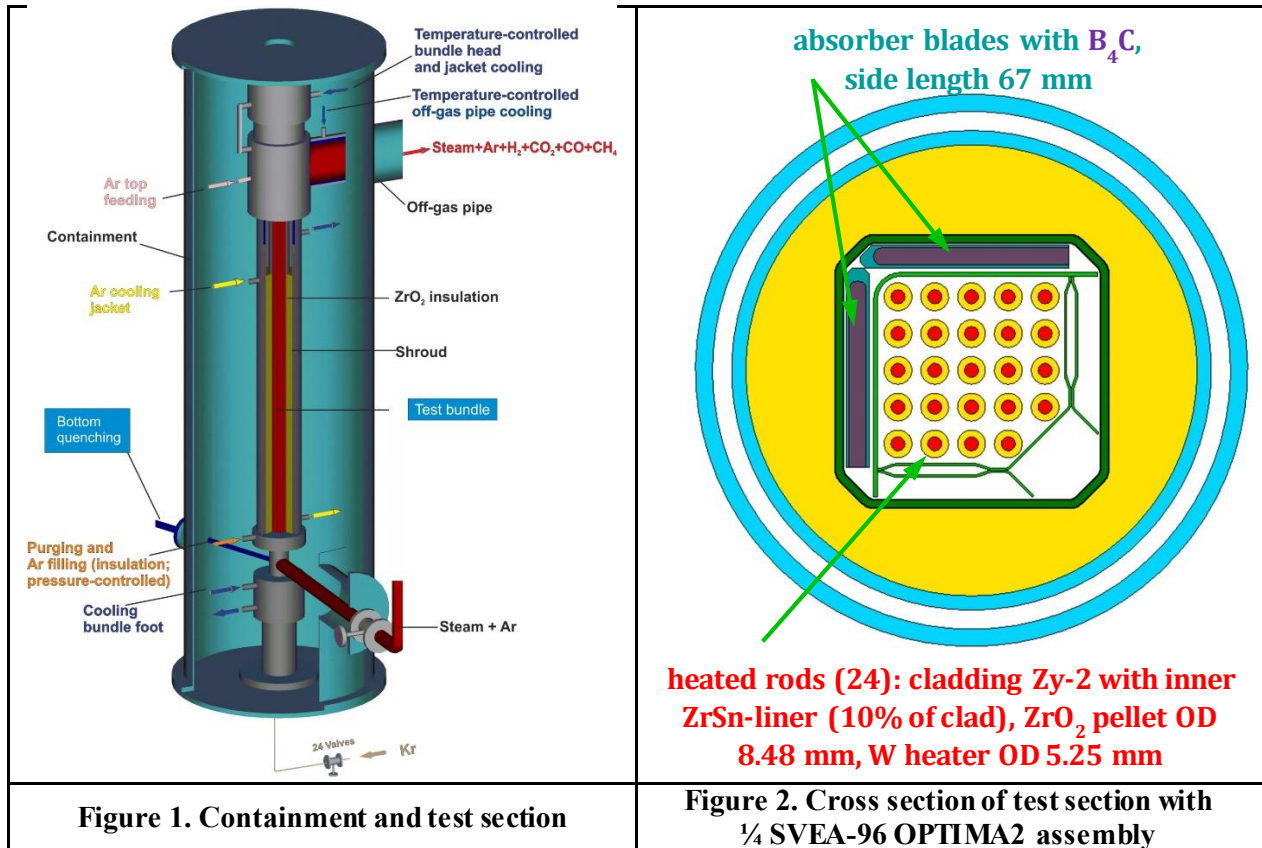


Figure 1. Containment and test section

Figure 2. Cross section of test section with 1/4 SVEA-96 OPTIMA2 assembly

The test bundle is approximately 2.5 m long and is made up of 24 heated fuel rod simulators. Heating is electric by 5.25 mm diameter tungsten heaters installed in the rod centers, and the bundle section heated by tungsten heaters between bundle elevations 0 and 1024 mm. Molybdenum heaters and copper electrodes are connected to the tungsten heaters at one end and to the cable leading to the DC electrical power supply at the other end. The tungsten heaters are surrounded by annular ZrO_2 pellets simulating UO_2 fuel. The Mo heaters and Cu electrodes are coated with ZrO_2 layer (about 200 μm thickness) to avoid an electrical contact to the cladding inner surface. All the test rods were filled with Kr at a overpressure of approximately 0.35 MPa after bundle heating to cladding peak temperature of 900 K. The system pressure maintained at about 0.2 MPa. The fuel rod simulators are held in position by five grid spacers at bundle elevations -200, 50, 550, 1050 and 1410 mm. All five grid spacers were the standard Westinghouse Inconel X750 spacers. Two steelblades with horizontal B_4C absorber pins were filled with helium (0.12 MPa) and inserted between channel box and shroud. The composition of the steel blade is the following (low carbon alloy AISI 316L SS): Fe, Cr (17%), Ni(11%), Mo (2.5%), [Si, P, S (<1%)]. One corner rods was installed in the water channel and was designed to be withdrawn from the bundle to check the amount of oxidation and hydrogen absorption at specific time. This corner rod was withdrawn at the end of pre-oxidation stage.

The test bundle is surrounded by an octagonal shroud of Zr 702, then by ZrO_2 fiber insulation extending from the bottom (-300 mm) to the upper end of the heated zone (+1024 mm) and a double-walled cooling

jacket of Inconel 600 (inner)/stainless steel (outer) over the entire length. The annulus between shroud and cooling jacket with the fiber insulation is purged (after several cycles of evacuation) and then filled with stagnant argon. This annulus is connected to a flow- and pressure-controlled argon feeding system in order to keep the pressure constant at the target of 0.3 MPa (beyond this pressure gas is released by feeding system). It must prevent an access of steam from the test bundle to the annulus after possible shroud failure, after which argon is supplied continuously. The 6.7 mm annulus of the cooling jacket is cooled by argon from the upper end of the heated zone to the bottom of the bundle and by water in the upper electrode zone. Both the absence of ZrO₂ insulation above the heated region and the water cooling are to avoid too high temperatures of the bundle in that region.

For temperature measurements the test bundle, shroud, and cooling jackets are equipped with thermocouples. The thermocouples attached to the outer surface of the rod cladding at elevations between -250 and 1350 mm are designated “TFS” for all heated rods. The shroud thermocouples (designation “TSH”) are mounted at the outer surface between -250 and 1250 mm. The thermocouples installed at the blade side at the bundle elevations 250, 350 and 450 mm are designated as TBL. The thermocouples mounted at the channel box at elevations 350 and 450 mm are designated as TCH.

The release of gas species is analyzed by a quadrupole mass spectrometer Balzers “GAM300” located at the off-gas pipe of the test facility. The ion currents representing the concentrations of the respective gases are determined. From these data the mass production rate of hydrogen as well as of the other gases is calculated with the ratio of the partial pressure of the particular gas and that one of argon (carrier gas) and multiplied by the argon flow rate through the test bundle.

3. EVENTS DURING TEST PERFORMANCE

In the QUENCH-20 experiment the test sequence can be distinguished in the following stages:

Pre-oxidation	0000 – 14416 s,
Heat-up	14416 – 15882 s,
Quench	15882 – 16375 s with water flow rate 50 g/s.

The scheme of test performance is depicted in Fig. 3.

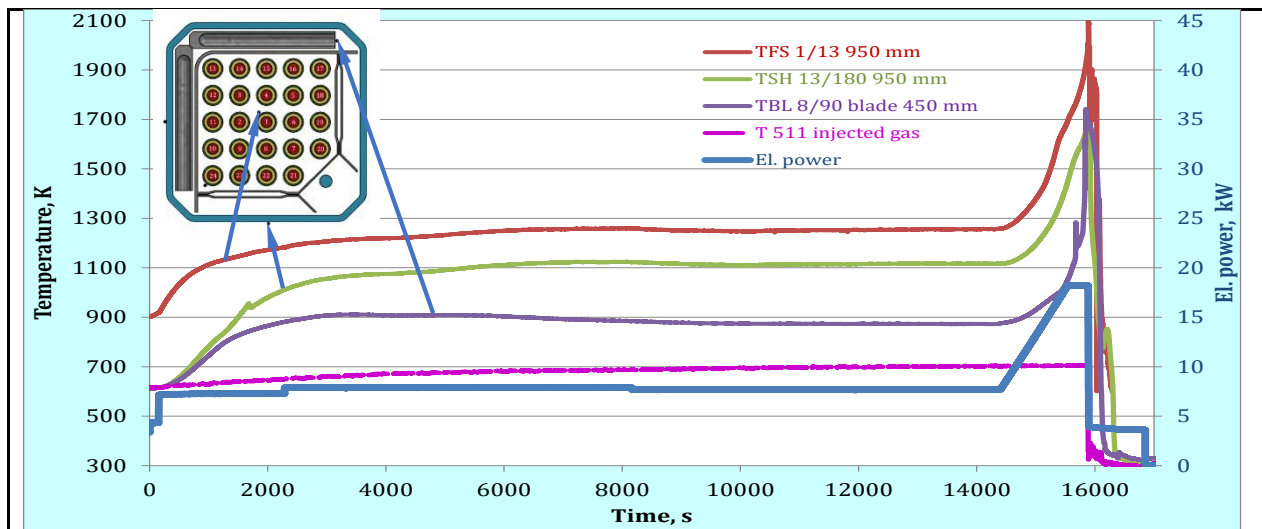


Figure 3. Test scenario

The hottest elevation of the QUENCH-20 was the level 950 mm similar to most former QUENCH bundle tests. To determine the axial temperature profile at a certain time, the average value of all thermocouple

readings of certain bundle elevation were calculated separately for claddings and shroud. Fig. 4 presents these axial temperature distributions on the end of the pre-oxidation stage and on the end of transient. For both time points, the hottest region was near to the elevation 950 mm. However, there is a significant temperature increase between 450 and 1050 mm during the transient stage.

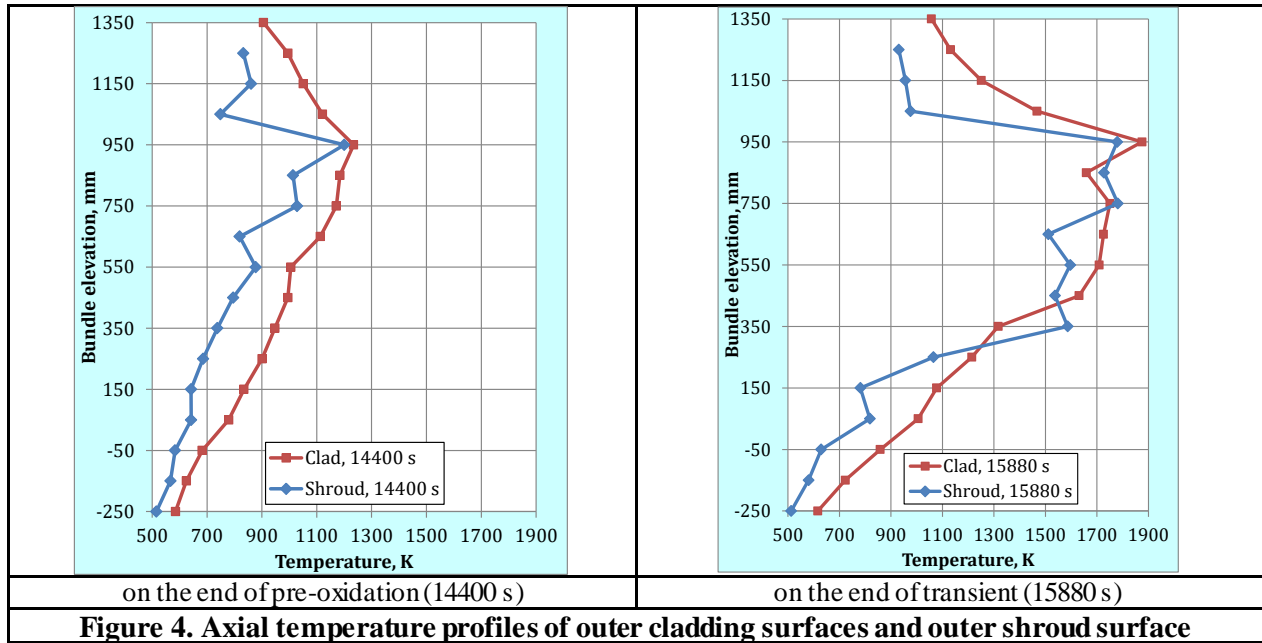


Figure 4. Axial temperature profiles of outer cladding surfaces and outer shroud surface

According to rod pressure drops, the cladding failures occurred during the transient stage, probably at temperature about 1700 K measured to the failure time point at the elevation 950 mm. Simultaneous release of Kr was registered by mass spectrometer, which shown seven Kr peaks corresponding to seven rod groups failed during about 200 s. In the first group, the rods 8, 1, and 4 of internal group were failed. The last group consists of rods 17 and 12 located at bundle periphery. The failure sequence from internal to outer rods; this is due to the radial temperature profile, decreasing from the center rod to the shroud. The absorber blade failures were registered by He release. The corresponding absorber melt relocations to the elevations of 250...450 mm were indicated during the transient stage by the TBL thermocouple installed at these elevations (Fig. 5).

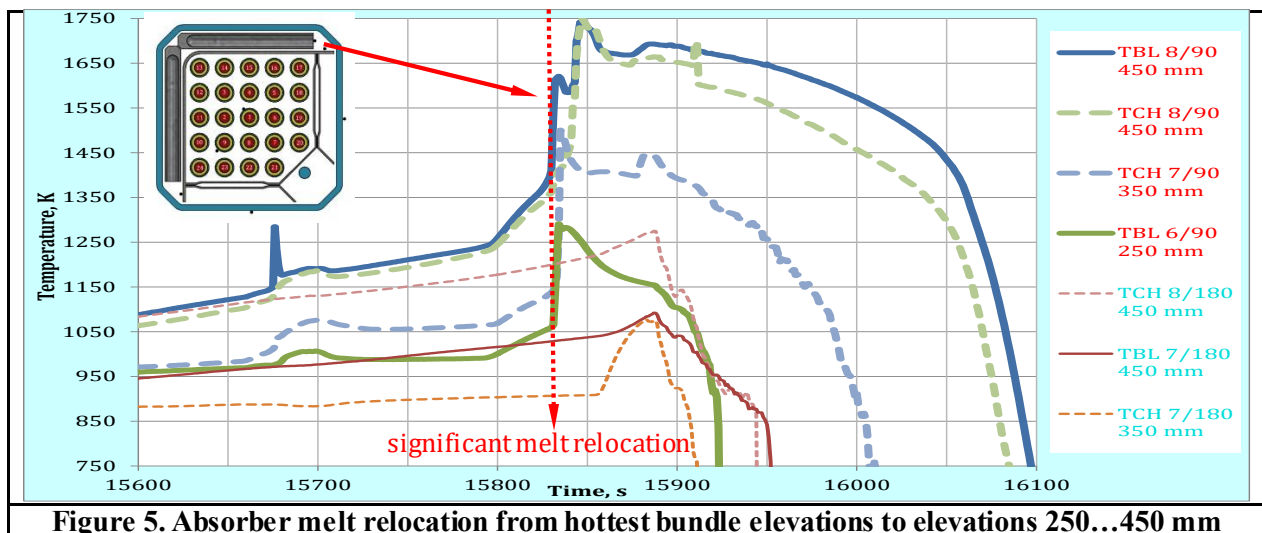
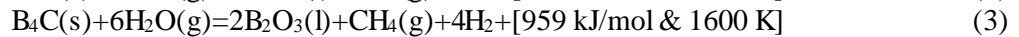
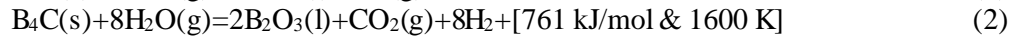
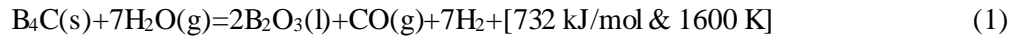


Figure 5. Absorber melt relocation from hottest bundle elevations to elevations 250...450 mm

The quench water injection was initiated at 15891 s. The maximum cladding temperature achieved during the test was recorded with the TFS 1/13 thermocouple at the time of quenching and amounted to 2098 K. During the quench stage, mass spectrometer registered release of following products of B₄C oxidation by steam: significant amounts of CO (12.6 g), and CO₂ (9.7 g) as well as relative small mass of CH₄ (0.4 g). This corresponds to following chemical reactions:



Steam reacts with liquid boron oxide to form volatile boric acids:

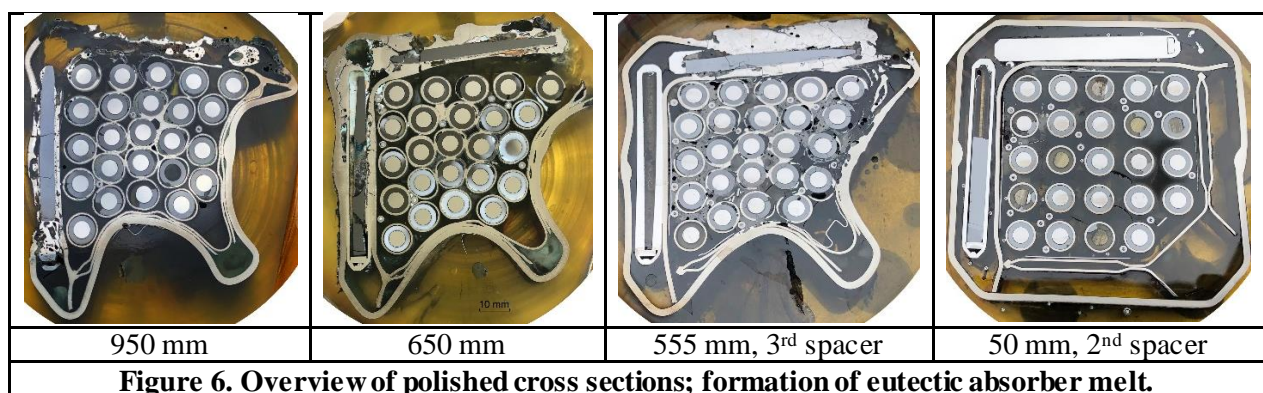


Boron oxide self directly evaporates temperatures above 1500 °C

The calculations, based on the relations (1)...(3) and measured data, showed that the corresponding mass of reacted B₄C was 38.4 g (4.3% from the total mass of B₄C pins), and additionally to released CO (12.6 g), CO₂ (9.7 g) and CH₄ (0.4 g) gases were formed 96.8 g B₂O₃ and released 10 g hydrogen. The total energy release due to boron carbide oxidation is about 500 kJ. The integral hydrogen release registered by mass spectrometer during the whole test was 57.4 g, from that 32 g during the quench stage.

4. METALLOGRAPHIC EXAMINATION

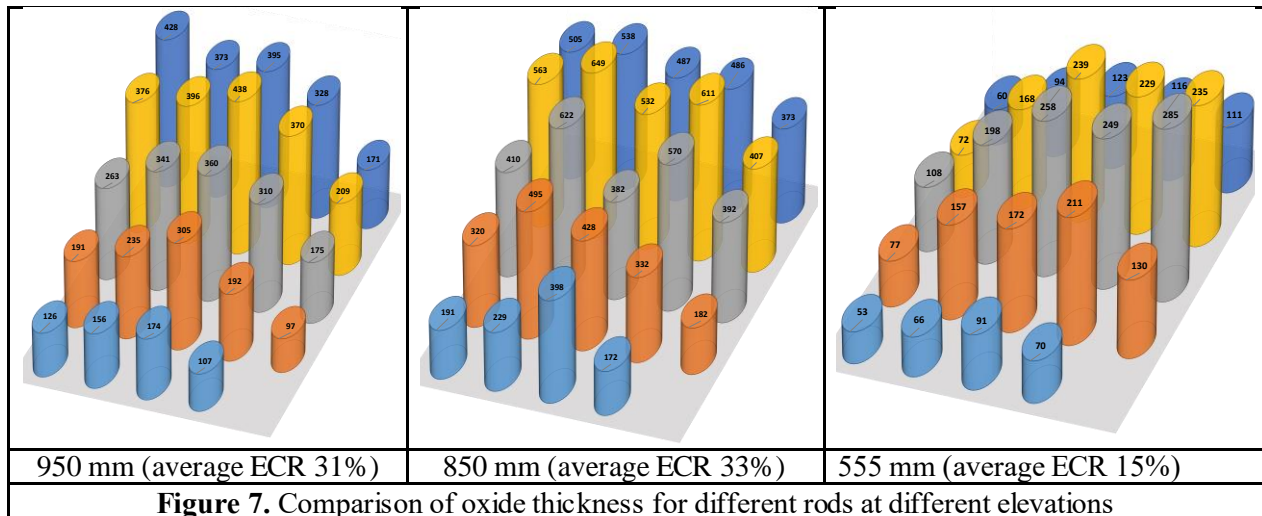
The test bundle was encapsulated in epoxy resin. After epoxy hardening during about three weeks, the bundle was cut into slices. Fig. 6 shows top views of grinded and polished cross sections between elevations 50 and 950 mm. The cladding melt was partially released into the space between rods at the bundle elevations 555...950 mm, whereas the eutectic absorber melt at elevations 450...950 mm.



The shroud was ductile deformed at angle positions 90° and 180° at bundle elevations above 350 mm due to higher gas pressure outside the shroud. This caused squeezing of bundle and two grid spacers (at 550 and 1050 mm) in directions to 0° and 270° and led to the narrowing of the cooling channels between the rods.

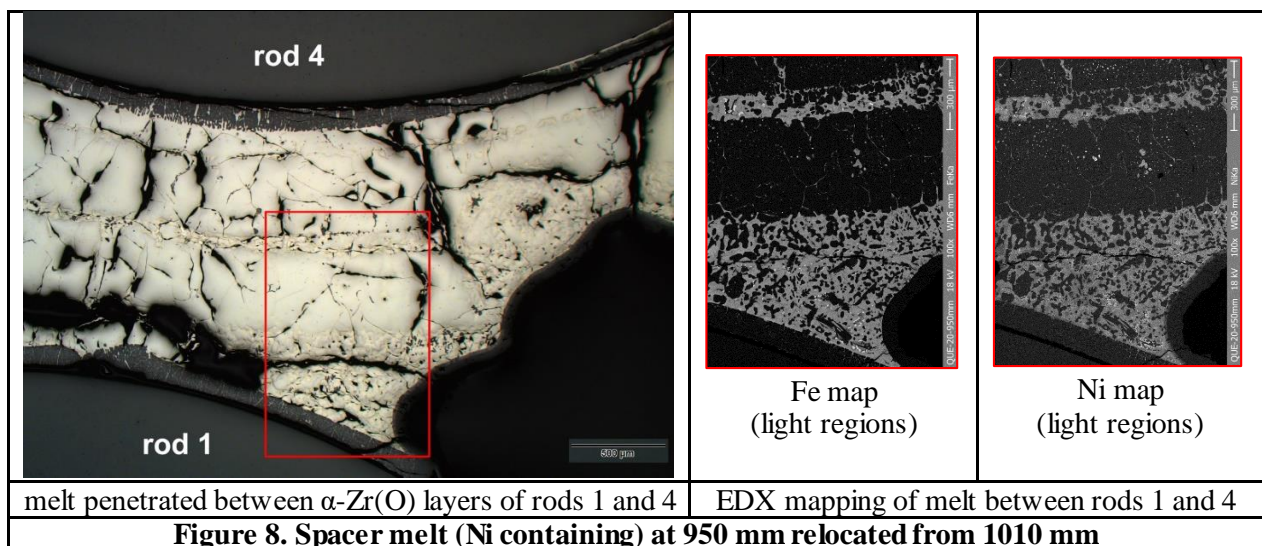
At elevations 1050 and 555 mm, only small fragments of Inconel spacer grids remained on the periphery of the bundle. At four contact points of spacer cell to cladding, the spacer grids at these elevations could melted locally due to the eutectic interaction of Ni of the grids with Zr of the claddings at about 1480 K. However, the main part of spacers was melted at the end of the transient (melting point of Inconel X-750 is 1610 K).

At the elevations of 450...950 mm, a detailed measurement of all characteristic layers of each cladding was carried out. Fig. 7 presents a comparison of the thicknesses of the outer oxide layers of all claddings at three bundle elevations.

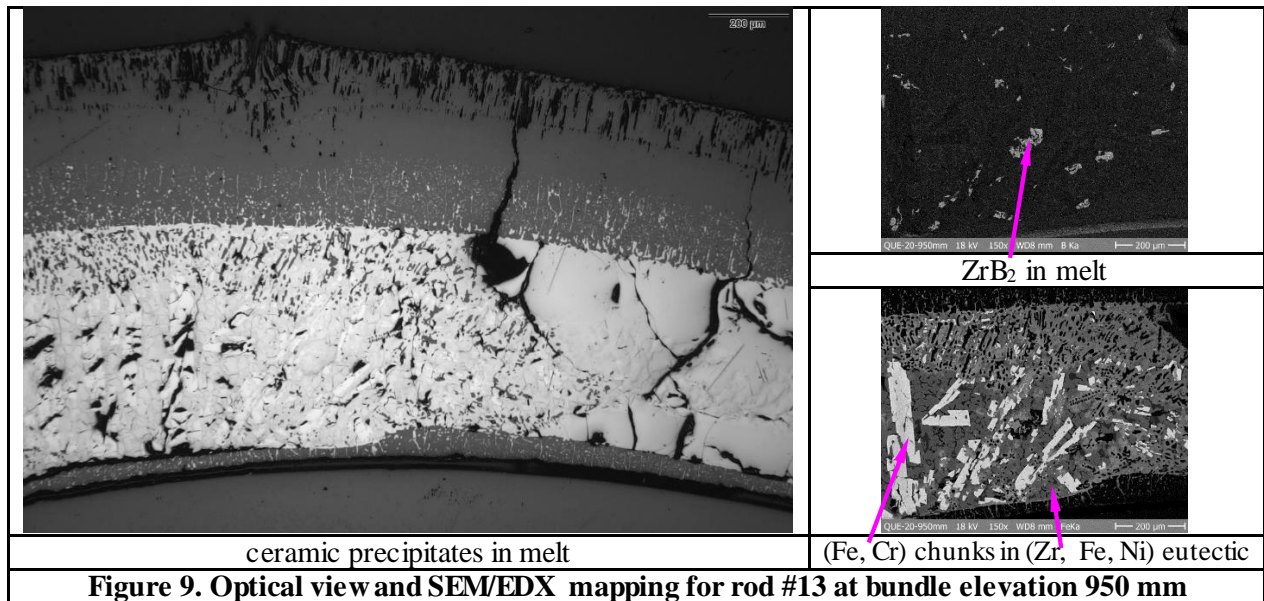


4.1. Elevation 950 mm

The peak cladding temperature about 2100 K was measured at the central rod during the quench stage. The absorber blade at the angle position 0° is strongly destroyed due to eutectic interactions. The B₄C pin is practically absent at this position, whereas the B₄C pin at the angle position 270° was only not significantly attacked by melt formed due to interaction of stainless steel blade with Zr-based cannel box and shroud. Small molten pools were formed around the central rod by cladding melt released through the failed oxide layers of claddings. This cladding melt is mixed with spacer melt relocated from 1050 mm and steel melt from absorber blades. The gap between pellets and cladding was increased (lift-off) during the pre-oxidation stage due to rod inner overpressure of Kr. The cladding melt was partially released outside the claddings of inner rods 1...9 and mixed with spacer melt and absorber steel melt. The spacer melt from 1050 mm and from the steel absorber plate has penetrated between α-Zr(O) layers of rods (Fig. 8). The inner cladding surface of several rods was also partially oxidized due to steam penetration in the gap or due to interaction with pellet.

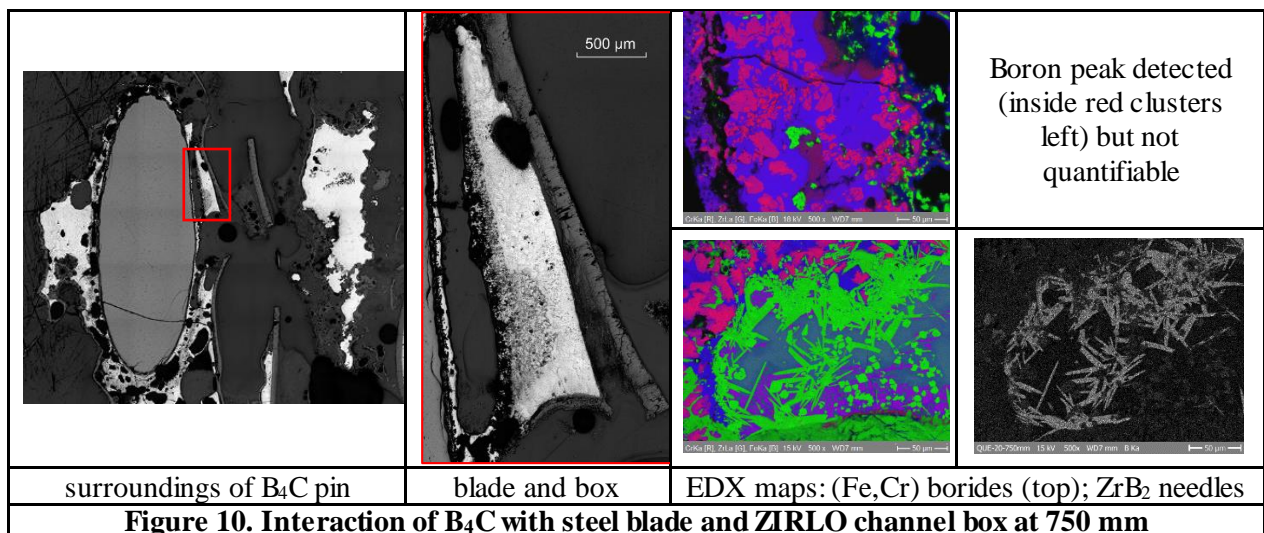


The claddings of peripheral hot rods along the absorber blades were strongly oxidized and partially melted. The claddings of rods 13, 14 and 15 were failed at the contact with water channel and absorber blade. The corresponding Zr/SS eutectic melt, containing ZrB₂ and (Fe, Cr) chunks, penetrated under cladding and distributed along the entire perimeter of the cladding under the outer oxide layer (Fig. 9). Part of the oxide layer was dissolved and formed ceramic precipitates in the melt. The phenomenology of this process was investigated and described in [9]. The claddings of the relatively cold peripheral rods (e.g. rod #20) were only moderately oxidized without melting. The water wings and the shroud were also only moderately oxidized in this relatively cold region.



4.2. Elevation 750 mm

Similar to 950 and 850 mm, the B₄C pin inside the absorber blade reacted with stainless steel of the absorber blade and partially dissolved (Fig. 10). The detailed SEM/EDX analysis of the eutectic melt around the B₄C pin revealed formation of equiaxed (Fe, Cr) borides near to pin and the needle-shape ZrB₂ near to Zr-based channel box, in full accordance with the structures observed in [7].



The cladding melt released inside the group of inner rods #1...#9 formed several molten pools with steam channels with oxidized edges. The pellet-cladding gaps of inner rods #1...#4 were filled with molten cladding metal or the voids were formed here due to downwards melt relocation. For the more cold inner rods #5...#9, the gaps were mostly free from the melt. For the hot peripheral rods #10...#17, the eutectic melt (formed due to interaction of stainless steel blades with ZIRLO bundle parts) filled the entire gap and contacted the pellet (Figs. 11, 12). The presence of zirconium borides in the melt of these claddings confirms the penetration of melted elements of the absorber blade under the outer oxide layer of claddings (Fig. 13). For the relatively cold peripheral rods #18...#22, the gap (formed during the lift-off of the cladding due to Kr overpressure) was free from the melt. The claddings of the last two peripheral rods #23 and #24, which are in turn in the hot bundle area, were partially melted (especially for rod #24), and the melt contacted pellet and the outer oxide layer.

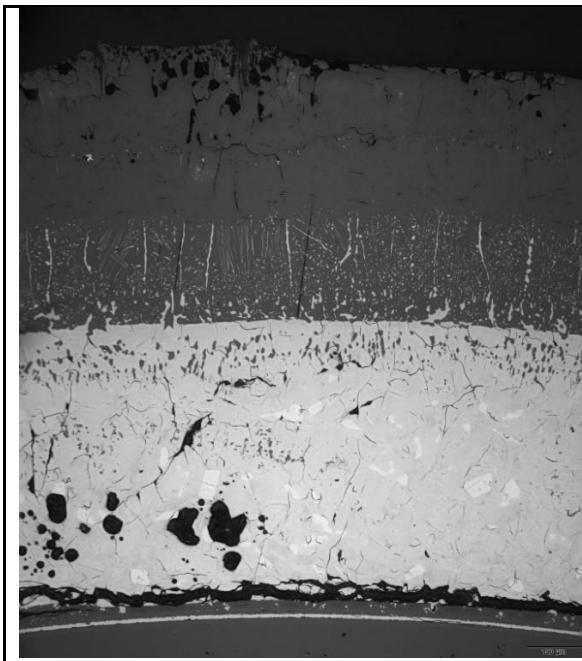


Figure 11. Microstructure of cladding #12 at bundle elevation 750 mm, 0°: few (Fe,Cr) chunks in the eutectic Zr/steel melt

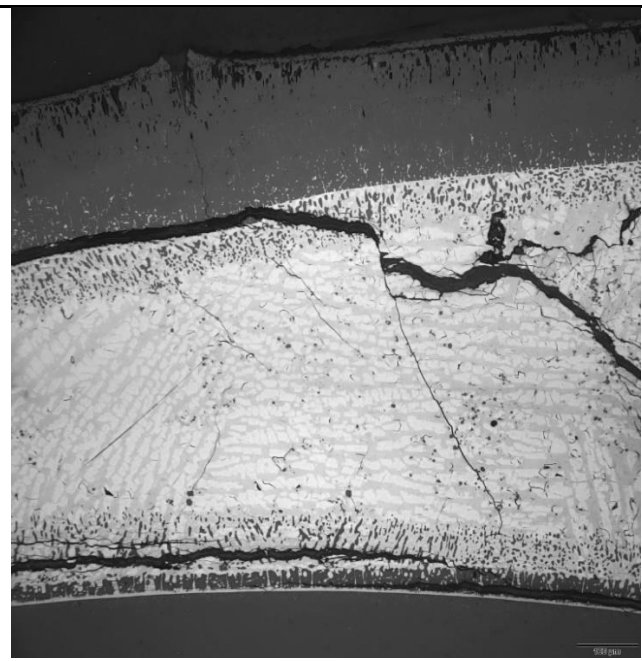
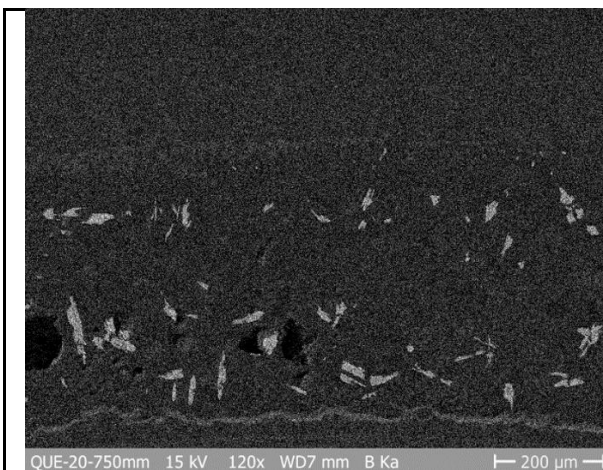
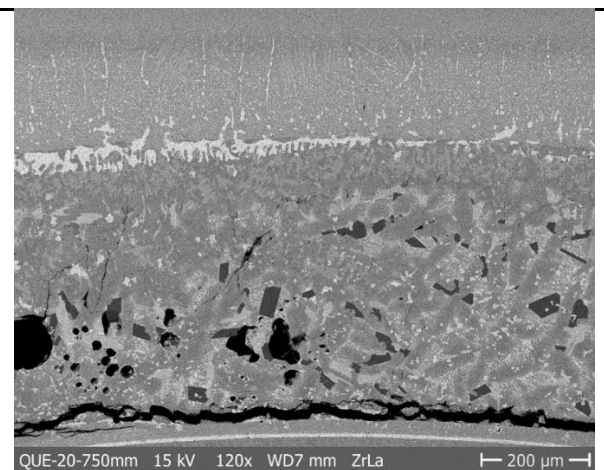


Figure 12. Microstructure of cladding #17 at bundle elevation 750 mm, 45°: numerous (Fe,Cr) chunks in the eutectic Zr/steel melt



B map

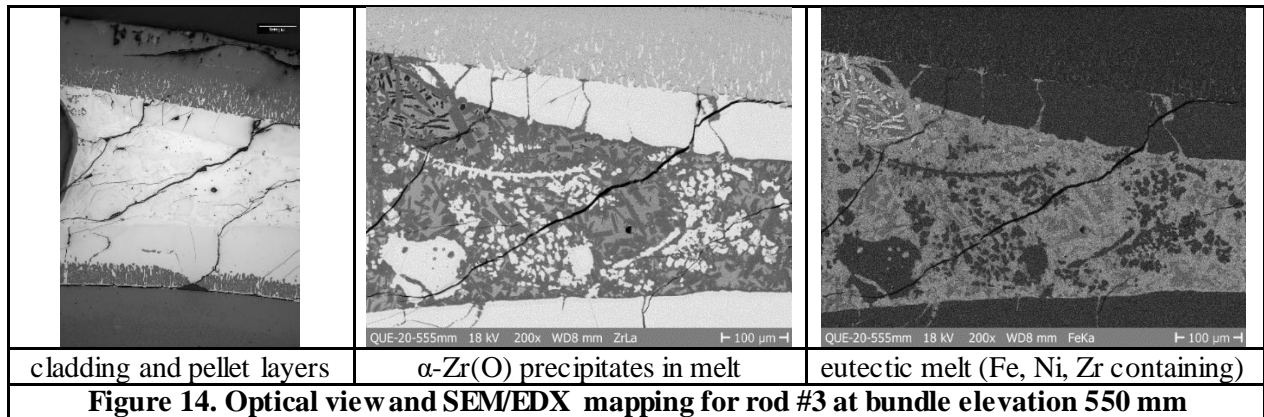


Zr map

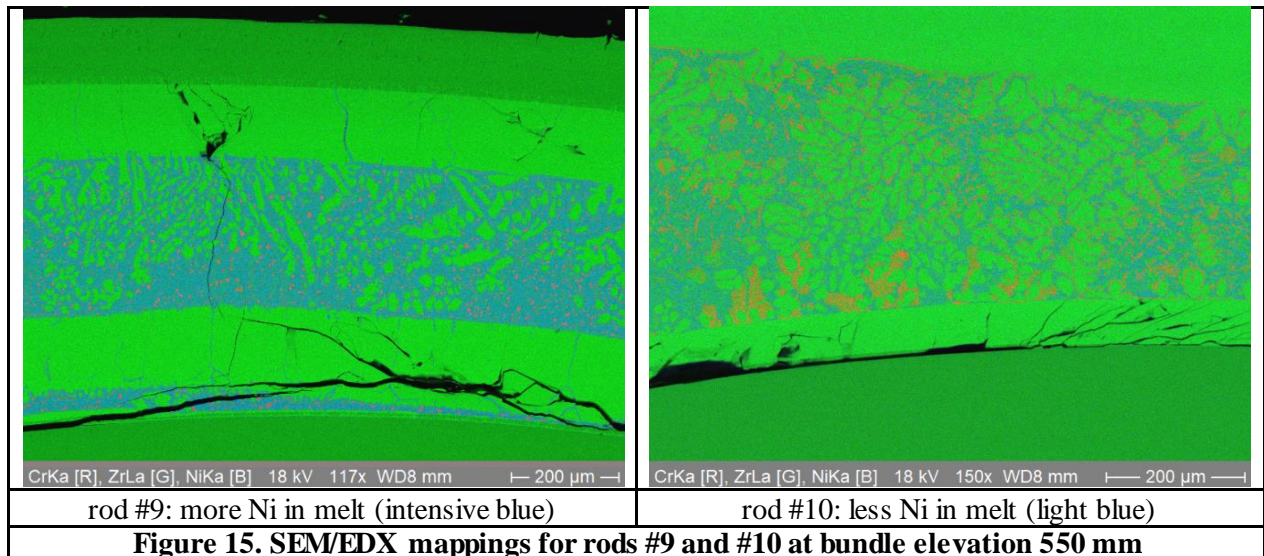
Figure 13. SEM/EDX mapping of zirconium borides in the eutectic melt of rod #12 at 750 mm

4.3. Elevation 550 mm

Temperature peaks on the shroud (azimuthal side 0°) during the transient indicate the relocation of the Zr-SS eutectic melt here from the upper bundle elevations. The interaction of the melt with the B₄C pins was minimal. Cladding oxidation was moderate and more pronounced in the center of the bundle. Only small fragments of Inconel spacer grids (about 70% Ni) remained on the periphery of the bundle. In the center of the bundle, the spacer grids at these elevations were melted firstly due to the eutectic interaction of the nickel of the grids with the zirconium of the claddings: the deepest eutectic temperature is 1233 K. At a later stage of the transient, the melting point of the Inconel spacer (1610 K) was exceeded. The melt partially relocated down, and partially penetrated under the damaged claddings (Fig. 14). This melt characterized by the formation of Zr precipitates distributed over the eutectic melt.



The claddings of the outer rods were less damaged than those of the inner ones, but the eutectic melt formed here was penetrated into the gap and distributed between inner and outer α -Zr(O) layers too. It is interesting to note that if the zirconium-nickel eutectic prevails in the melt for the hotter and more damaged inner rods, then the zirconium-iron-chromium eutectic dominates in the less damaged outer rods. This is clear too seen from the comparison of the SEM/EDX analysis of rods 9 and 10 (Fig. 15). Sometimes for the outer rods, the formation of (Fe, Cr) chunks in the (Zr, Ni) eutectic melt is observed.



5. CONCLUSIONS

Experiment QUENCH-20 with BWR geometry simulation bundle was successfully conducted at KIT on 9th October 2019 in the framework of the international SAFEST project. The test bundle mock-up represented one quarter of a BWR fuel assembly with 24 electrically heated fuel rod simulators and two B₄C control blades. The rod simulators were filled with Kr to inner pressure of 5.5 bar at peak cladding temperature of 900 K. The pre-oxidation stage in the flowing gas mixture of steam and argon (each 3 g/s) and system pressure of 2 bar lasted 4 hours at the peak cladding temperature of 1250 K. The Zry-4 corner rod, withdrawn at the end of this stage, showed the maximal oxidation at elevations between 930 and 1020 mm with signs of breakaway. During the transient stage, the bundle was heated to a maximal temperature of 2000 K. The coolability of bundle was decreased by its squeezing due to the shroud ductile deformation caused by overpressure outside the shroud. The cladding radial extensions and failures due to inner overpressure (about 4 bar) were observed at temperature about 1700 K and lasted about 200 s.

During the period of rod failures also the first absorber melt relocation accompanied by shroud failure were registered. The interaction of B₄C with steel blade and ZIRLO channel box was observed at elevations 650...950 mm with formation of eutectic melt. The typical components of this melt are (Fe, Cr) borides and ZrB₂ precipitated in steel melt or in Zr-steel eutectic melt. Massive absorber melt relocation was observed 50 s before the end of transition stage. Small fragments of the absorber melt moved down to the elevation of 50 mm. The melting point of Inconel spacer grids at 500 and 1050 mm was reached also at the end of the transition stage. The Inconel melt from the elevation 1050 mm relocated downwards through hot bundle regions to the Inconel grid spacer at 550 mm and later (during the escalation caused by quench) to 450 mm. This melt penetrated also under damaged cladding oxide layer and formed molten eutectic mixtures between elevations 450 and 550 mm.

The test was terminated with the quench water injected with a flow rate of 50 g/s from the bundle bottom. Fast temperature escalation from 2000 to 2300 K during 20 s was observed. As result, the metal part (prior β -Zr) of claddings between 550 and 950 mm was melted, partially released into space between rods and partially relocated inside the gap between pellet and outer oxide layer to 450 mm. It should be noted the positive role of the oxide layer, which does not allow the melt to completely escape into the inter-rod space - and thereby limiting the possibility of interaction of a large amount of melt with steam, which could significantly increase the exothermic oxidation processes and the escalation of temperatures.

The distribution of the oxidation rate within each bundle cross section is very inhomogeneous: whereas the average outer ZrO₂ layer thickness for the central rod (#1) at the elevation of 750 mm is 465 μ m, the same parameter for the peripheral rod #24 is only 108 μ m. The average oxidation rate of the inner cladding surface (due to interaction 1) with steam, 2) with pellets) is about 20% in comparison to the outer cladding oxidation. The bundle elevations 850 and 750 mm are *mostly* oxidized with average cladding ECR 33% due to: 1) downwards shift of the temperature maximum from 950 mm (ECR 31%) during transient and quench, 2) due to cladding melt relocation inside and outside the rods from 800...1000 mm to lower bundle elevations. The oxidation of the melt relocated inside rods was observed at elevations 550...950 mm.

The mass spectrometer measured release of CO (12.6 g), CO₂ (9.7 g) and CH₄ (0.4 g) during the reflood as products of absorber oxidation; corresponding B₄C reacted mass was 41 g or 4.6% of total B₄C. It is significantly lower than in the PWR bundle tests QUENCH-07 and QUENCH-09 containing central absorber rod with B₄C pellets inserted into a thin stainless steel cladding and Zry-4 guide tubes (20% and 50% reacted B₄C correspondingly [5]). Hydrogen production during the reflood amounted to 32 g during the reflood (57.4 g during the whole test) including 10 g from B₄C oxidation.

ACKNOWLEDGMENTS

The QUENCH-20 experiment was performed in the framework of the SAFEST project in cooperation with Swedish Radiation Safety Authority (SSM), Westinghouse Sweden, GRS and KTH and supported by the KIT program NUSAFE. Personal thanks to Mr. Isaksson (SSM), Mr. Bechta (KTH), Mr. Hollands (GRS), Ms. Korske (Westinghouse) for their help and fruitful cooperation. The bundle materials and absorbers were provided by Westinghouse Sweden. The authors thank particularly J. Moch (KIT) for bundle preparation

REFERENCES

1. J. Stuckert, M. Steinbrueck, M. Grosse, “Experimental program QUENCH at KIT on core degradation during reflooding under LOCA conditions and in the early phase of a severe accident,” *Proceedings of Meeting on Modelling of Water Cooled Fuel Including Design Basis and Severe Accidents*, Chengdu/China, 28 October–1 November 2013, IAEA-TECDOC-CD-1775, pp. 281-297, https://www-pub.iaea.org/MTCD/Publications/PDF/TE-1775_CD_web.pdf (2013).
2. T. Haste, M. Steinbrück, M. Barrachin, O. de Luze, M. Grosse, J. Stuckert, “A comparison of core degradation phenomena in the CORA, QUENCH, Phébus SFD and Phébus FP experiments,” *Nuclear Engineering and Design*, **283**, pp. 8–20 (2015), <https://doi.org/10.1016/j.nucengdes.2014.06.035>.
3. M. Steinbrück, M. Große, L. Sepold, J. Stuckert. “Synopsis and outcome of the QUENCH experimental program”, *Nuclear Engineering and Design*, **240** (7), pp. 1714-1727, (2010), <https://doi.org/10.1016/j.nucengdes.2010.03.021>.
4. M. Steinbrück, C. Homann, A. Miassoedov, G. Schanz, L. Sepold, U. Stegmaier, H. Steiner, J. Stuckert. „Results of the B₄C control rod test QUENCH-07“, *FZKA-6746* (2004), <https://doi.org/10.5445/IR/270058023>.
5. M. Steinbrück, A. Miassoedov, G. Schanz, L. Sepold, U. Stegmaier, H. Steiner, J. Stuckert. „Results of the QUENCH-09 experiment with a B₄C control rod“, *FZKA-6829* (2004), <https://doi.org/10.5445/IR/270059406>.
6. P. Hofmann, M. Markiewicz, J. Spino. “Reaction Behaviour of B₄C Absorber Material with Stainless Steel and Zircaloy in Severe LWR Accidents”, *KfK 4598*, CNEA NT -10/89, (1989), <https://doi.org/10.5445/IR/270027893>.
7. M. Steinbrück. “Degradation and oxidation of B₄C control rod segments at high temperatures”, *Journal of Nuclear Materials*, **400** (2), pp. 138-150, (2010), <https://doi.org/10.1016/j.jnucmat.2010.02.022>.
8. J. Stuckert, M. Große, J. Laier, J. Moch, U. Peters, U. Stegmaier, M. Steinbrück. „Results of the QUENCH-20 experiment with BWR test bundle“, *NUSAFE 3576* (2022).
9. P. Hofmann, J. Stuckert, A. Miassoedov, M.S. Veshchunov, A.V. Berdyshev, A.V. Boldyrev. “ZrO₂ dissolution by molten zircaloy and cladding oxide shell failure. New experimental results and modelling”, *FZKA-6383*, <https://doi.org/10.5445/IR/270046616>.